Phosphorylation and activity of the tumor suppressor Merlin and the ERM protein Moesin are coordinately regulated by the Slik kinase

Sarah C. Hughes[1] and Richard G. Fehon[2]

[1]Department of Cell Biology, University of Alberta, Edmonton, Alberta T6G 2H7, Canada
[2]Department of Molecular Genetics and Cell Biology, University of Chicago, Chicago, IL 60637

Merlin and Moesin are closely related members of the 4.1 Ezrin/Radixin/Moesin domain superfamily implicated in regulating proliferation and epithelial integrity, respectively. The activity of both proteins is regulated by head to tail folding that is controlled, in part, by phosphorylation. Few upstream regulators of these phosphorylation events are known. In this study, we demonstrate that in *Drosophila melanogaster*, Slik, a Ste20 kinase, controls subcellular localization and phosphorylation of Merlin, resulting in the coordinate but opposite regulation of Merlin and Moesin. These results suggest the existence of a novel mechanism for coordinate regulation of cell proliferation and epithelial integrity in developing tissues.

Introduction

The maintenance of epithelial integrity is closely integrated with the regulation of cell proliferation in a variety of biological contexts, including normal development, tissue regeneration, and tumor progression. During mammalian development, there is close linkage between regulation of the cell cycle and the ability of neural crest progenitors to delaminate from the neurepithelium and initiate migratory behavior (Kalcheim and Burstyn-Cohen, 2005). In addition, epithelial wounding produces a local stimulation of proliferation as a result of the disruption of cell contacts (Bryant and Simpson, 1984; Johnston and Gallant, 2002). Most importantly, recent studies have revealed that a number of neoplastic tumor suppressor mutations result simultaneously in the disruption of epithelial polarity, tissue integrity, and normal controls on proliferation. For example, loss of the *Drosophila melanogaster* tumor suppressor gene *scribble* results in highly disorganized cell masses that display uncontrolled proliferation (Bilder et al., 2000; Zeitler et al., 2004). The underlying basis for the observed tight linkage between epithelial organization and cell proliferation remains unclear, but current models include cell contact–mediated mechanisms for growth arrest, compartmentalized distribution of growth factors, their receptors, and/or intracellular transducers, and the existence of components that have dual but separable roles in epithelial integrity and cell signaling (for example, β-catenin; Bilder, 2004). These studies highlight the importance of cellular architecture, particularly the cytoskeleton and its ability to organize the cell membrane through linkage with transmembrane proteins, to regulate both epithelial integrity and proliferation.

The neurofibromatosis 2 tumor suppressor protein Merlin and its close relatives Ezrin/Radixin/Moesin (ERM; Trofatter et al., 1993b; Bretscher et al., 2002) function as membrane-cytoskeletal linkers and regulators of multiple signaling pathways (Shaw et al., 2001; Bretscher et al., 2002; Speck et al., 2003). Merlin and ERMs share ∼45% sequence identity and a similar domain organization with an N-terminal 4.1 ERM domain, a putative coiled-coil spacer, and a C-terminal domain that in ERMs binds to filamentous actin (Bretscher et al., 2002). Merlin has a clear role in regulating proliferation (Rouleau et al., 1993; Trofatter et al., 1993a), whereas Moesin and its paralogues Ezrin and Radixin are thought to maintain epithelial integrity by organizing the apical cytoskeleton (Speck et al., 2003).

A central question in the study of these proteins has been how their interaction with binding partners is regulated. For both Merlin and ERMs, there is abundant evidence for an intramolecular interaction between the 4.1 ERM domain and the C-terminal domain (Gary and Bretscher, 1995; Sherman et al., 1997; Gonzalez-Agosti et al., 1999; Gronholm et al., 1999; Meng et al., 2000; Nguyen et al., 2001). In ERM proteins, this interaction produces a closed, inactive form of the protein that does not interact with either transmembrane binding partners

Correspondence to Richard G. Fehon: rfehon@uchicago.edu

Abbreviations used in this paper: ERM, Ezrin/Radixin/Moesin; kd, kinase dead; MARCM, mosaic analysis with a repressible cell marker; PAK, p21-activated kinase; Thr, threonine; UAS, upstream activation sequence.

The Journal of Cell Biology, Vol. 175, No. 2, October 23, 2006 305–313
http://www.jcb.org/cgi/doi/10.1083/jcb.200608009

or filamentous actin (Matsui et al., 1998; Nakamura et al., 1999). For Merlin, studies in mammalian cells suggest that the closed form is active in inhibiting proliferation (Sherman et al., 1997; Shaw et al., 1998; Gutmann et al., 1999; Morrison et al., 2001), whereas studies in *Drosophila* suggest that, as with ERMs, the open form of Merlin retains all essential genetic functions (LaJeunesse et al., 1998). Whether this apparent distinction between flies and mammals represents a true functional difference or reflects methodological differences remains to be resolved.

Phosphorylation of a conserved threonine (Thr) in the actin-binding domain of ERM proteins has been demonstrated to be important for their activation by relieving the head to tail interaction (Nakamura et al., 1995; Matsui et al., 1998; Oshiro et al., 1998; Hayashi et al., 1999; Tran Quang et al., 2000). The precise kinase responsible for this event is unclear, although its activity seems to be positively regulated by Rho activation in mammalian cells. In *Drosophila*, the Ste20 family kinase Slik is necessary for the phosphorylation of Moesin, although, again, it is not clear whether Slik phosphorylates Moesin directly or via intermediate kinases (Hipfner et al., 2004). In mammalian cells, Merlin activity is regulated by a phosphorylation event at serine 518 that blocks head to tail interactions (Shaw et al., 2001). However, unlike ERMs, it appears that the phosphorylated form of Merlin is inactive in that it does not suppress growth (Shaw et al., 2001). In contrast, hypophosphorylated Merlin is enriched under conditions of serum starvation or confluency, suggesting that this form is growth suppressive (Sherman et al., 1997; Shaw et al., 1998; Gutmann et al., 1999). Serine 518 is thought to be phosphorylated by the p21-activated kinase (PAK) downstream of Rac activity (Kissil et al., 2002; Xiao et al., 2002), although the possibility of other mechanisms regulating Merlin phosphorylation cannot be excluded. In addition, evidence to date has failed to demonstrate phosphorylation of the equivalent Thr residue to the one phosphorylated in ERMs, although this residue is conserved in both mammalian and fly Merlin.

Many questions remain about the regulation of Merlin activity, particularly in the context of developing tissues undergoing normal proliferation. To better understand how Merlin is regulated, we have investigated the mechanism by which Merlin phosphorylation and, thus, its activity are controlled in *Drosophila*. In particular, we have examined the possibility that Merlin and Moesin are regulated by the same molecular mechanism. In this study, we show that Slik kinase, which positively regulates Moesin function, also regulates Merlin but in the opposite direction. In addition, our observations suggest a competitive interaction between Moesin and Merlin for Slik activity. These results provide in vivo evidence of a kinase-based regulation of *Drosophila* Merlin and suggest that Merlin and Moesin are coordinately regulated in developing tissues.

Results

Merlin subcellular localization is dependent on Slik function

Previous studies in *Drosophila* and mammalian cells have demonstrated that Merlin displays complex subcellular localizations, being found both at the apical plasma membrane and in punctate cytoplasmic structures that are associated with endocytic compartments (McCartney and Fehon, 1996; Scherer and Gutmann, 1996; Schmucker et al., 1997; Kissil et al., 2002). Deletion mutagenesis indicates that the C-terminal domain is important in regulating Merlin's subcellular localization and its activity in rescue assays (LaJeunesse et al., 1998). This domain is similar in structure to the C-terminal domain of ERM proteins, and, although it does not bind actin, the Thr residue that is phosphorylated in ERMs is conserved in both fly and human Merlin (McCartney and Fehon, 1996). Collectively, these observations raise the possibility that the phosphorylation state and, therefore, Merlin subcellular localization and function are modulated similarly to Moesin. A previous study has shown that the phosphorylation of *Drosophila* Moesin is regulated by the Ste20 family kinase Slik and that like Moesin and Merlin, Slik is localized in the apical region of epithelial cells (Hipfner et al., 2004). Based on these observations, we investigated possible functional interactions between Slik and Merlin.

To examine the effect of the loss of Slik function on Merlin subcellular localization, we used FLP/FRT (Flip recombinase/Flip recombination target)-mediated mitotic recombination to generate clones of $slik^{-/-}$ cells in heterozygous $slik^{-/+}$ (wild type) imaginal epithelia. Induction of a homozygous *slik* mutant clone by mitotic recombination simultaneously produces a homozygous wild-type ($slik^{+/+}$) sister clone, thus allowing side by side comparisons between cells containing two, one, or no functional copies of the *slik* gene. Wild-type cells within the epithelium are positively marked by the expression of either one copy ($slik^{-/+}$) or two copies ($slik^{+/+}$) of a GFP transgene, whereas $slik^{-/-}$ cells lack this marker. Optical sections taken below the apical surface of the epithelium (Fig. 1, A–A″) show a clear inverse correlation between *slik* gene dosage and Merlin staining. Merlin staining was increased in homozygous $slik^{-}$ clones and decreased in homozygous wild-type sister clones relative to the surrounding heterozygous $slik^{-/+}$ cells.

To extend this result, we next asked whether the apparent increase in Merlin staining in $slik^{-}$ clones might reflect altered subcellular localization. Specifically, we wondered whether Merlin, which is normally localized primarily to the apical junctional region in imaginal epithelial cells, might be redistributed basally in $slik^{-}$ cells. Such redistribution might reflect an altered phosphorylation state for Merlin, as has been observed for the ERM proteins (Bretscher et al., 2002). For this experiment, we fixed tissues using a TCA treatment that has previously been shown to preserve the phosphorylation state in mammalian ERM proteins (Hayashi et al., 1999). Our initial experiments indicated that this protocol considerably enhanced detection of the phosphorylated form of Moesin and confirmed the previous report that Moesin phosphorylation is dependent on Slik activity (Fig. 1, B and B′; Hipfner et al., 2004). In these preparations, phospho-Moesin staining was decreased both in apical (Fig. 1 B′) and basolateral (Fig. 1 C′) optical sections. Consistent with our initial observations, we observed obviously increased levels of Merlin protein throughout the basolateral part of $slik^{-}$ epithelial cells (Fig. 1 C″). In stark contrast, Merlin staining in

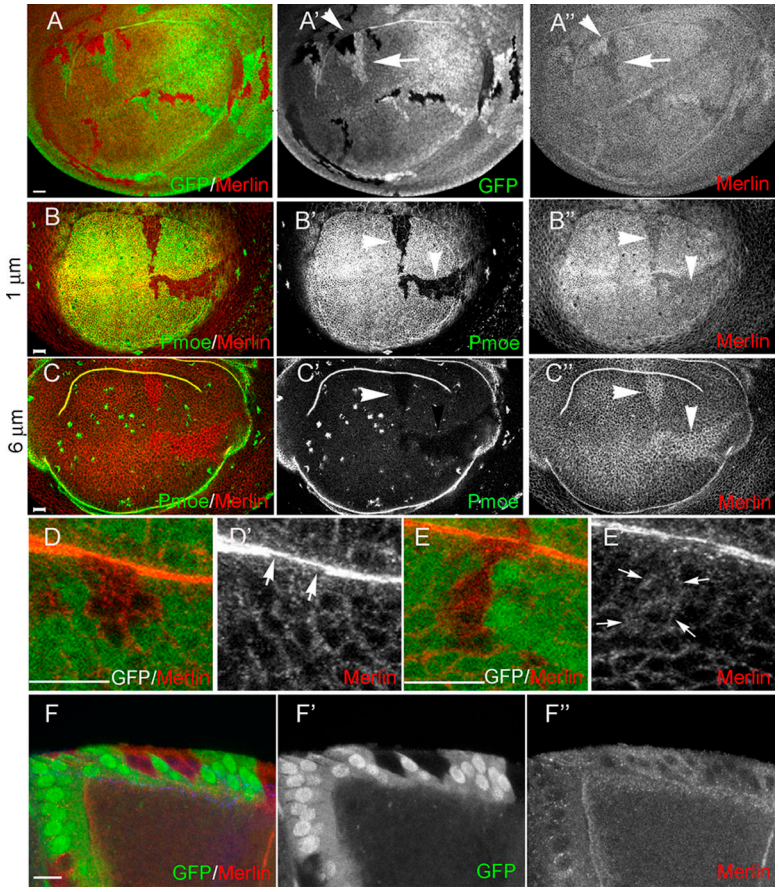

Figure 1. **Slik activity affects Merlin protein localization in a dose-dependent manner.** Mitotic clones of *slik*^{1} mutant cells are marked by the lack of a GFP marker (A′, arrowhead; and D, E, and F′) or the lack of phospho-Moesin (B′ and C′, arrowheads). (A–A′′) Sections taken below the apical surface show a marked increase in Merlin staining within homozygous *slik*^{1} clones (A′′, arrowhead), with a concomitant decrease in Merlin staining within the wild-type sister clone (A′′, arrow) marked by the increased expression of GFP (A′, arrow). (B–C′′) Optical sections taken either 1 (B–B′′) or 6 µm (C–C′′) beneath the apical surface demonstrate that in *slik*^{1} clones, Merlin is mislocalized away from the apical surface. An apical section (B′′, arrowheads) shows decreased Merlin staining in the *slik*^{1} clone, whereas more basal Merlin staining is increased in *slik*^{1} cells (C′′, arrowheads). (D–E′) Optical cross sections of clones showing the reduction of Merlin apically (D′, arrows) and an increase in punctate Merlin staining basally (E′, arrows). (F–F′′) A similar effect on Merlin protein staining and localization are seen in the follicle cell epithelium surrounding the developing oocyte. Bars, 10 µm.

slik^{-} clones was decreased at the apical surface of the epithelium, where much of the protein is normally found (Fig. 1 B′′). Similar results were also observed using standard PFA fixation in optical cross sections through clones (Fig. 1, D and E). In addition, these sections suggest that much of the basolateral Merlin staining in *slik*$^{-}$ cells is associated with punctate structures (Fig. 1, D′ and E′). Thus, the loss of Slik function results in a redistribution of Merlin from a close association with the apical membrane to the basolateral domain of the cell. Similar effects are also observed in clones induced in the follicle cell epithelium that surrounds the developing oocyte (Fig. 1, F–F′′).

Slik affects Merlin localization and trafficking in cultured cells

To further examine the effects of Slik activity on Merlin subcellular localization, we performed coexpression experiments in cultured *Drosophila* S2 cells. Previous studies (McCartney and Fehon, 1996; LaJeunesse et al., 1998) have shown that upon induction, Merlin initially localizes to the membrane of S2 cells and then, within 3 h, traffics into punctate cytoplasmic structures that are associated with endocytic vesicles (McCartney and Fehon, 1996). Perturbation of the C-terminal domain of Merlin alters its localization and trafficking pattern (LaJeunesse et al., 1998). To determine whether Slik affects the subcellular localization and movement of Merlin, a pulse-chase assay was performed in S2 cells using a heat shock–inducible GFP-tagged Merlin expression construct (LaJeunesse et al., 1998). Control experiments in which cells were induced to express a pulse of Mer^{+} exhibited a similar pattern of Merlin localization to that reported previously (Fig. 2, B–E; LaJeunesse et al., 1998). In contrast, the coexpression of Slik with Mer^{+} results in a shift in the temporal pattern of Merlin localization. In this case, a substantial proportion of cells displayed Merlin that associated with the plasma membrane even 6 h after induction (Fig. 2, A and F). Thus, Slik activity prevents the normal trafficking of Merlin off the plasma membrane and into cytoplasmic punctate structures. Coexpression of a kinase-inactive version of Slik has no effect on Merlin localization or trafficking (Fig. 2, compare G with E). Together with the loss of function clonal analysis, these results indicate that Slik kinase activity controls the localization and trafficking of Merlin.

Slik regulates Merlin phosphorylation

Given the documented role of Slik in Moesin phosphorylation (Hipfner et al., 2004) and the high degree of structural homology between Merlin and Moesin (Bretscher et al., 2002), we reasoned that the alteration in Merlin subcellular localization in *slik*$^{-}$ clones and S2 cells could reflect changes in its phosphorylation state. Therefore, we used immunoprecipitation and immunoblot analysis to examine Merlin phosphorylation under varying levels of Slik activity. Previous studies in mammalian cells have shown that Merlin exists in several isoforms, representing at least two and, under certain conditions, three phosphorylated states (Shaw et al., 1998, 2001). *Drosophila* Merlin

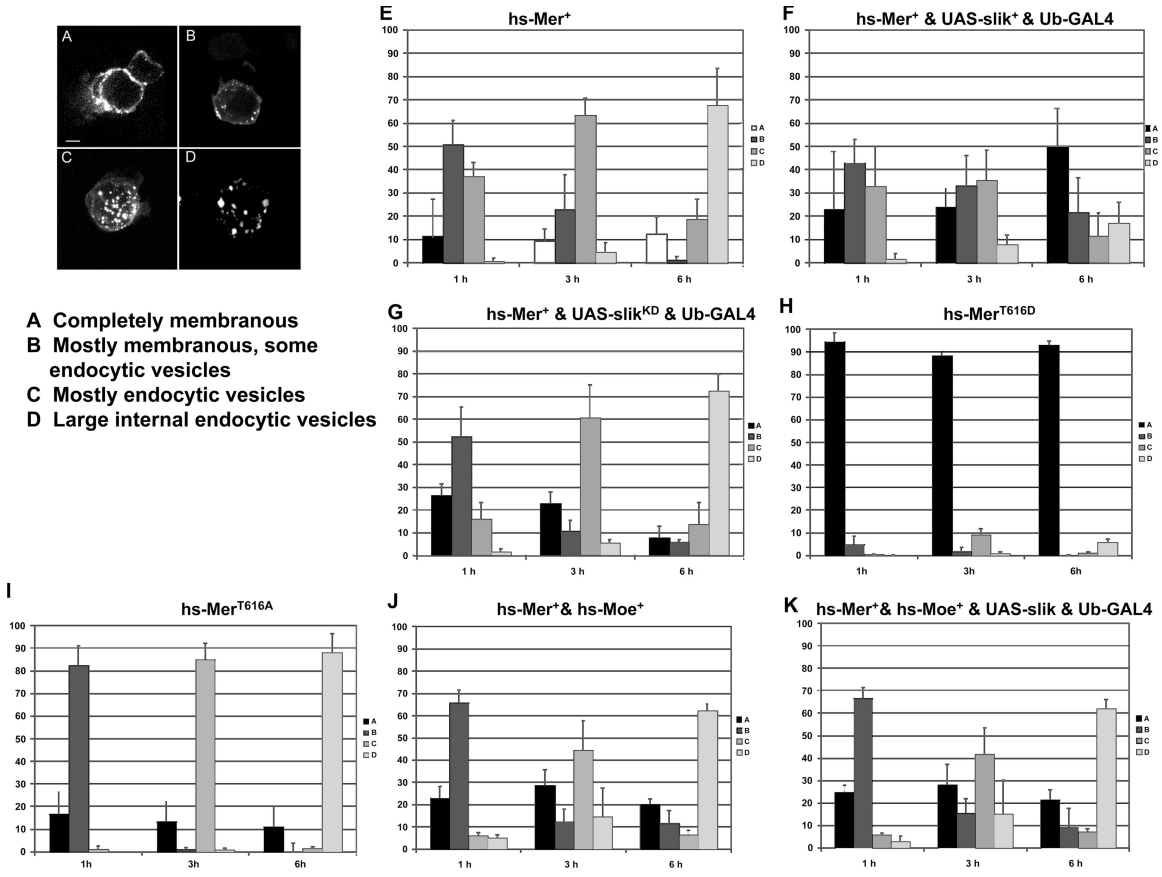

Figure 2. **Slik activity alters the subcellular localization and trafficking of Merlin protein in S2 cells.** (A–D) Different subcellular localizations of Merlin are observed after transient expression using a short pulse of heat shock–driven expression of GFP-tagged Merlin (hs-Mer^{+}GFP). (A) High levels of Merlin protein localized completely at the membrane. These levels are increased from what is seen with a pulse of Merlin expression alone. (B) Moderate levels of mostly membranous Merlin localization with a small number of cytoplasmic punctate structures. (C) Merlin localized to numerous small cytoplasmic vesicles throughout the cell. (D) Merlin localized to fewer, larger cytoplasmic vesicles. (E–K) Histograms of cells displaying various phenotypes (in A–D) at different time points (1, 3, and 6 h) after Merlin expression. The y axis corresponds to the percentage of each phenotype observed in the field of cells counted. Error bars indicate SD of at least three replicates. (E) Trafficking of wild-type Merlin. A progression from the plasma membrane to large endocytic vesicles is observed over time as previously described (McCartney and Fehon, 1996; LaJeunesse et al., 1998). (F) Merlin trafficking in cells that express both Merlin and Slik. There is a slower progression of Merlin moving from the plasma membrane into cytoplasmic vesicles. In addition, there is an increase in the number of cells exhibiting high levels of Merlin that remain at the membrane (A). (G) Cells in which both Merlin and Slik^{kd} are expressed. Merlin localization in these cells is very similar to that observed in cells expressing Merlin alone (E). (H) A phosphomimetic form of Merlin, Mer^{T616D}, is retained at the plasma membrane for an extended time compared with Mer^{+}. (I) Nonphosphorylatable Merlin (Mer^{T616A}) traffics away from the plasma membrane faster than Mer^{+}. (J) Merlin coexpressed with wild-type Moesin trafficking similarly to Merlin expression alone (E). (K) Merlin trafficking in cells that express Merlin, Moesin, and Slik. Merlin localization patterns are similar to the expression of Merlin alone (E). Bar, 2 μm.

produces a similar pattern on immunoblots (Fig. 3 A), where at least three forms can be visualized. Treatment with λ phosphatase converted the slower migrating bands to the most rapidly migrating form (Fig. 3 B), indicating that the slower migrating forms represent differentially phosphorylated forms of the protein.

When *upstream activation sequence* (*UAS*)–*slik* was expressed in wing imaginal discs under the apterous GAL4 driver, the ratio of phosphorylated to nonphosphorylated Merlin increased compared with wild-type imaginal discs (6.3 ± 1.6 vs. 4.3 ± 0.7; $n = 6$; $P = 0.009$). In contrast, Merlin isolated from wing discs that overexpressed kinase-inactive Slik showed a phosphorylation pattern that was indistinguishable from wild type (ratio of phosphorylated to nonphosphorylated = 4.6 ± 1.0; $n = 4$; $P = 0.44$; Fig. 3 A). This indicates that kinase activity of Slik is required for the observed effect on the phosphorylation of Merlin protein.

To better characterize Slik effects on Merlin phosphorylation, we next examined these proteins when expressed in *Drosophila* cultured S2 cells. A similar pattern of Merlin isoforms is observed on immunoblots when Merlin is expressed in S2 cells, as was seen in wing imaginal discs (unpublished data). Increased phosphorylation of Merlin in the presence of Slik kinase is also observed in S2 cells, albeit with a more subtle effect.

As the Thr residue near the C terminus of Moesin (Thr^{559}) is also conserved in Merlin (Thr^{616}; McCartney and Fehon, 1996), we wondered whether Slik activity might control the phosphorylation of this site in Merlin. To address this question, we used site-directed mutagenesis to construct phosphomimetic (Mer^{T616D}) and nonphosphorylatable (Mer^{T616A}) versions of the Merlin protein and examined their effect on Merlin phosphorylation in the presence of Slik kinase in S2 cells.

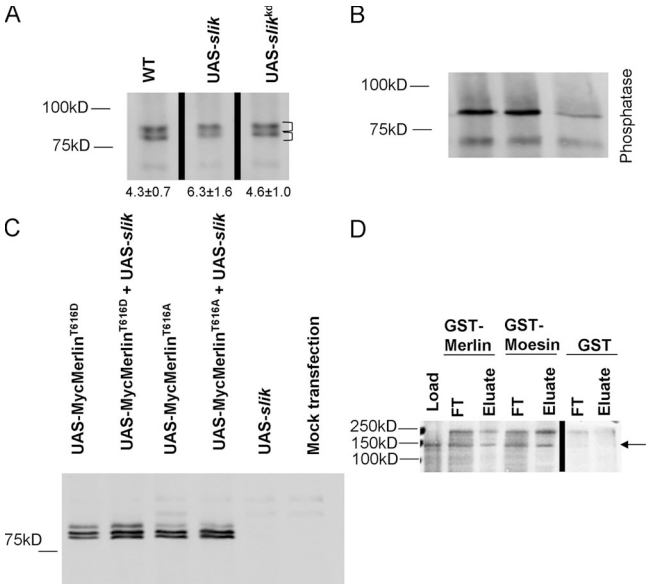

Figure 3. **Slik activity can alter Merlin phosphorylation.** (A) Merlin protein was immunoprecipitated from third instar imaginal disc cell lysates. Merlin protein migrates as two prominent bands and one or more minor bands in wild-type (WT) lysates. Numbers below the lanes represent the ratio of the top (phosphorylated) bands to the bottom (unphosphorylated) band in each lane (top bracket vs. the bottom bracket). For wild type and *UAS-slik*, $n = 6$, and for *UAS-slik*^{kd}, $n = 4$. In cell lysates from imaginal discs in which Slik is overexpressed (*UAS-slik*), the more hyperphosphorylated (slower migrating) bands are relatively more abundant, as evidenced by the increased ratio of top to bottom bands. Expression of the kinase-inactive Slik (*UAS-slik*^{kd}) has a similar phosphorylation pattern to wild type. All samples in this blot are from the same experiment but have been rearranged for order. (B) To confirm that the shift observed in migration of the Merlin bands is caused by phosphorylation, samples were treated with λ phosphatase. All Merlin staining is reduced to a single species after this treatment. The samples in this blot are representative examples taken from a separate experiment than that shown in A. In this case, the *UAS-slik*^{kd} sample was under loaded. (C) The phosphorylation patterns of Mer^{T616D} and Mer^{T616A} in the presence or absence of coexpressed Slik kinase in S2 cells. The slowest migrating form of Mer^{T616D} is enhanced relative to Mer^{T616A}. Neither pattern is altered by the coexpression of Slik. (D) In vitro GST pull-down assay showing a direct interaction between the S^{35}-labeled Slik protein (arrow) and both GST-Merlin and GST-Moesin but not with GST alone. This blot is taken from a single experiment. A background band above Slik is also present in the GST control. FT, flow through.

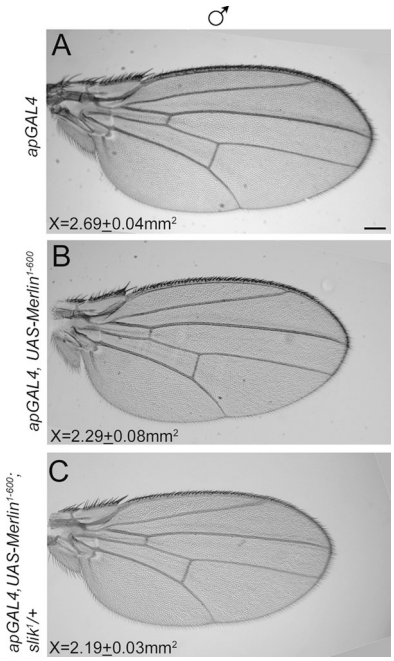

Figure 4. **Slik activity inhibits Merlin function genetically.** The phenotypic modification of an activated Merlin protein (Mer$^{1-600}$) by reduction in Slik function was analyzed. (A) A representative example of a male wild-type wing from flies carrying the *apGAL4* driver, which is expressed in the dorsal surface of the wing. (B) A representative example of a wing in which activated Merlin (Mer$^{1-600}$) is expressed in the dorsal surface of the wing under the *apGAL4* driver. There is a mean 15% decrease in wing area from the wild type. (C) Removal of one copy of *slik*^{1} in the wings expressing Mer$^{1-600}$ produces a further reduction in wing area by a mean of 18% from the wild type. Thus, reduction of Slik function enhances the activated Merlin phenotype. Measurements in each panel represent the mean area of the wing (millimeters squared) for each genotype. For each combination, at least 10 wings were measured. Bar, 200 μm.

Expressed Mer^{T616D} displays a prominent hyperphosphorylated band, whereas this band is much less prominent in expressed Mer^{T616A} (Fig. 3 C). These results indicate that sites in addition to Thr^{616} are phosphorylated in Merlin and suggest that the phosphorylation state of Thr^{616} may regulate the phosphorylation of these sites by other kinases. The addition of Slik kinase does not appear to alter the phosphorylation pattern of either mutant (Fig. 3 C), which is consistent with the notion that Slik acts on Merlin via phosphorylation of the Thr^{616} residue.

If Slik's effects on Merlin localization are mediated by phosphorylation, phosphomimetic Merlin mutations should affect subcellular localization in a similar manner to the cotransfection of wild-type Merlin with Slik. To examine this, Mer^{T616D} and Mer^{T616A} were tested in the aforementioned S2 cell trafficking assay. As we observed for wild-type Merlin in the presence of Slik kinase (Fig. 2 F), Mer^{T616D} alone trafficked very slowly off the plasma membrane (Fig. 2 H). However, Mer^{T616A} internalized from the plasma membrane to the cytoplasm with even faster kinetics than Mer^{+} or Mer^{+} coexpressed with kinase-inactive Slik (Fig. 2, compare I with E and G). These results indicate that one effect of phosphorylation is to regulate Merlin trafficking and subcellular localization. They also suggest that phosphorylated Merlin remains closely associated with the plasma membrane, whereas hypophosphorylated Merlin rapidly traffics off of the membrane, possibly in association with transmembrane proteins.

To ask whether Slik interacts directly with Moesin and Merlin, we used an in vitro GST pull-down assay (Fig. 3 D). The results indicate that bacterially expressed Merlin and Moesin both bind to Slik in vitro. In addition, we attempted to determine whether purified Slik can phosphorylate either Moesin or Merlin in vitro. However, as previously shown for Moesin (Hipfner et al., 2004), we were unable to detect direct phosphorylation of Merlin or Moesin by Slik kinase (unpublished data). Whether this indicates that Slik acts in vivo via intermediary kinases or requires unidentified cofactors not present in our experiments is unknown, but the observation that Slik interacts directly with both Moesin and Merlin is consistent with the idea that they serve as substrates for Slik's kinase activity.

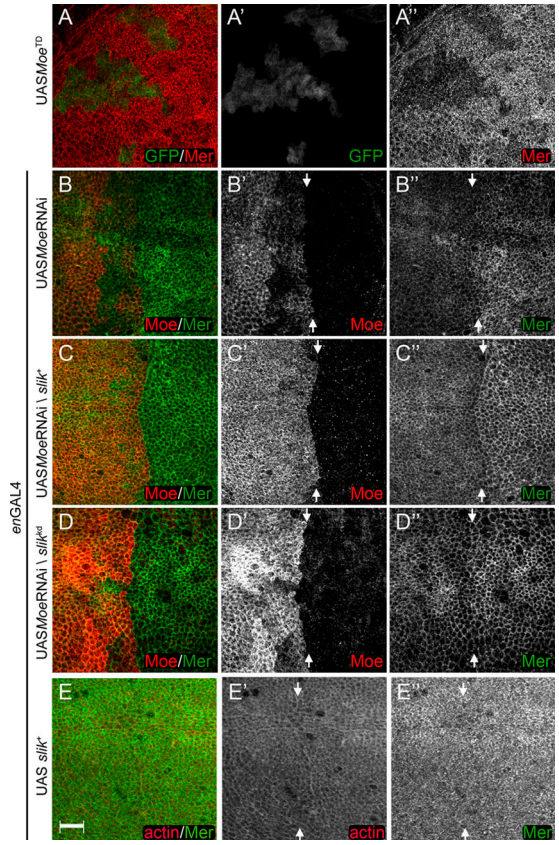

Figure 5. **Slik affects Merlin independently of Moesin.** The effect of Slik on Merlin was analyzed in the presence or absence of Moesin. (A–A′′) An activated Moesin (Moe^{T559D}) transgene was expressed in *slik*^{1} clones using the MARCM technique. Mutant clones are positively marked with GFP. Within *slik*^{1} clones, the expression of a constitutively active Moesin does not rescue the mislocalization of Merlin protein away from the apical membrane. (B–B′′) A Moesin RNAi transgene expressed under the control of the *enGAL4* driver in the posterior compartment produces a subtle increase in Merlin staining. (C–C′′) Coexpression of a Moesin RNAi transgene to knock down Moesin expression together with *UAS-slik* in posterior cells results in a clear increase in Merlin protein staining in the apical domain. Note that the boundary between the anterior and posterior compartments is clearly defined in C′′. (D–D′′) Coexpression of a Moesin RNAi transgene with *UAS-slik*^{kd} does not alter Merlin staining or localization, indicating that the kinase activity of Slik is required. (E–E′′) Expression of *UAS-slik* using *enGAL4* in the presence of normal levels of Moesin has no detectable effect on Merlin protein staining in the posterior compartment of a third imaginal wing disc. Arrows mark the anterior-posterior boundary, with posterior to the right. Bar, 10 μm.

Slik interacts genetically with Merlin

As a further test of functional interaction between Merlin and Slik, we examined genetic interactions between *Merlin* and *slik* mutations. Specifically, we asked whether reducing slik function genetically modifies the phenotype of an activated *Merlin* transgene (*Mer*$^{1\text{-}600}$; LaJeunesse et al., 1998) that confers growth suppression. The expression of *Mer*$^{1\text{-}600}$ in wild- type wings causes a reduction in size by a mean of 15% from wild type ($P = 0.01$; Fig. 4, A vs. B). Using this sensitized genetic background, we asked whether manipulating *slik* gene dose affects the activity of endogenously expressed wild-type Merlin. The reduction of *slik* dose (*slik* is completely recessive) by one half in this genetic background reduced wing size by a mean of 18% ($P = 0.002$; Fig. 4, A vs. C). Thus, reduction in Slik function enhances the phenotype from expressing an activated form of Merlin, suggesting that Slik antagonizes Merlin function. This phenotypic interaction is most likely mediated through Slik's effects on endogenously expressed wild-type Merlin acting synergistically with the coexpressed $Mer^{1\text{-}600}$, which lacks the Thr^{616} residue.

Is Slik regulation of Merlin independent of Moesin?

The evidence presented thus far supports a model whereby Slik controls Merlin subcellular localization and function by regulating its phosphorylation state. In this model, Slik directly affects Merlin function. Alternatively, it is possible that Slik alters Merlin activity indirectly through its previously documented effects on Moesin function (Hipfner et al., 2004). To address this question, we asked whether the expression of a phosphomimetic Moesin mutation, Moe^{T559D}, which has been shown to be active even in the absence of *slik* function (Hipfner et al., 2004), could rescue the effects of the loss of *slik* on Merlin subcellular localization (Fig. 1). For this experiment, we used the mosaic analysis with a repressible cell marker (MARCM) technique to express Moe^{T559D} specifically in *slik*$^{-}$ somatic mosaic clones. This technique allows the overexpression of one protein (Moe^{T559D}) while removing the expression of another protein (Slik) in the same set of cells. As shown in Fig. 5 A, the expression of activated Moesin does not reverse Merlin mislocalization away from the apical membrane in *slik*$^{-}$ cells, indicating that the effect of Slik on Merlin is not mediated through its effects on Moesin activation.

If Merlin and Moesin are substrates for Slik-dependent phosphorylation, one might predict that Moesin and Merlin act competitively for Slik activity. To address this, we examined the effect of Slik overexpression on Merlin localization in the apical domain in the presence or absence of Moesin protein. The expression of Slik alone under the control of the *en*GAL4 driver in the posterior compartment resulted in no discernable effect on Merlin (Fig. 5 E′′). To address the potential role of Moesin, we simultaneously reduced Moesin function using a transgene that produces double-stranded RNA for Moesin (Karagiosis and Ready, 2004). Reduction of Moesin expression using this RNAi transgene alone results in a subtle increase in Merlin protein staining in the apical domain (Fig. 5 B′′). However, the expression of wild-type Slik in combination with a reduction in Moesin produced a marked increase in Merlin protein staining in the apical domain (Fig. 5 C′′), indicating a shift toward increased apical localization. In contrast, coexpression of kinase-dead (kd) Slik ($Slik^{kd}$) and the Moesin RNAi transgene had no apparent effect on Merlin (Fig. 5 D′′), indicating again that Slik kinase activity is necessary for these effects.

We also addressed the relationship between Merlin and Moesin using the aforementioned S2 cell trafficking assay. Coexpression of Merlin and Moesin does not alter the subcellular trafficking of Merlin (Fig. 2, J vs. E). However, the coexpression of Moesin blocks the effect of Slik on Merlin trafficking (Fig. 2, compare E with K), which is consistent with the hypothesis that Moesin and Merlin act as competitive substrates.

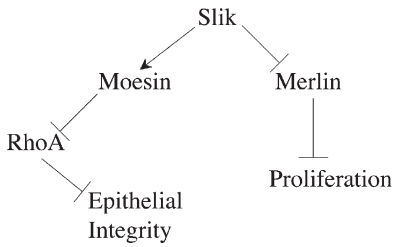

Figure 6. **Schematic diagram of functional relationships between Slik, Merlin, Moesin, and the regulation of tissue integrity and proliferation in developing epithelia.** As demonstrated in this study, Slik activity simultaneously promotes Moesin function and inhibits Merlin. Our previous results have shown that Moesin functions to negatively regulate Rho activity and promote epithelial integrity (Speck et al., 2003). Merlin functions to restrict proliferation in the same epithelia. Thus, the net result of Slik activity is to drive proliferation and simultaneously stabilize epithelial integrity.

Discussion

A previous study has shown that the Slik kinase positively regulates Moesin activity via phosphorylation near the C terminus, thereby inhibiting activation of the Rho small GTPase and promoting epithelial integrity (Hipfner et al., 2004). Overexpression of Slik in imaginal tissues results in the hyperphosphorylation of Merlin, suggesting that in addition to Moesin, Slik regulates the phosphorylation state of Merlin. Interestingly, in mammalian cells, Merlin phosphorylation is affected by PAK, which, like Slik, is a member of the Ste20 family of kinases (Dan et al., 2001). Current models of Merlin function predict that hyperphosphorylated Merlin is inactive (Bretscher et al., 2002), which is consistent with our observation that *slik* functions antagonistically to *Merlin* in genetic interaction tests. In accord with this notion, *slik* was originally identified in a misexpression screen by its ability to cause overproliferation when expressed ectopically in imaginal epithelia (Hipfner and Cohen, 2003). Collectively, the data presented here leads us to predict that activity of the Slik kinase coordinately regulates both epithelial morphology and, at the same time, cell proliferation (for summary see Fig. 6). To our knowledge, this is the first demonstration of a single mechanism with the potential to regulate both processes simultaneously in developing tissues.

We speculate that the observed coordinate regulation of Merlin and Moesin may be important in the developing imaginal discs during larval and pupal development. In larval stages, most imaginal epithelia proliferate rapidly and at the same time maintain a highly structured epithelial monolayer (Bilder, 2004). At this stage, Slik activity could allow high rates of proliferation and simultaneously promote epithelial integrity that is necessary to prevent the unregulated growth or invasive cell behavior. At the end of larval life and at the onset of metamorphosis, the cell cycle slows dramatically, and, at the same time, the imaginal discs radically change shape during a morphogenetic process termed eversion. Previous studies have shown that these shape changes require rearrangements of local contacts between cells (Condic et al., 1991; Irvine and Wieschaus, 1994; Goode and Perrimon, 1997), suggesting that epithelial integrity must be modulated. We predict that at this stage, Slik function may be decreased to coordinate these changes in the imaginal epithelium. Further studies to examine Slik expression and the regulation of its function will be of interest in this regard.

This study also provides the first genetic evidence that Moesin and Merlin functionally interact through competition for Slik kinase activity, although previous studies have shown physical interactions between these proteins (Gonzalez-Agosti et al., 1999; Gronholm et al., 1999; Meng et al., 2000). It is interesting to note that in mammalian Schwann RT4 cell lines, expressing constitutively phosphorylated Merlin not only impairs the ability of Merlin to suppress proliferation and motility but also induces a novel ERM-like phenotype (Surace et al., 2004). Surace et al. (2004) attribute this phenotype to the conversion of Merlin to an ERM-like molecule. However, if Merlin and Moesin are also coordinately regulated in mammalian cells, an alternative possibility is that overexpression of a phosphomimetic Merlin could affect the phosphorylation state of endogenous ERM proteins, thereby increasing their level of activity.

We found that the loss of *slik* function results in a dramatic shift in Merlin localization from the apical plasma membrane to punctate cytoplasmic structures. We have previously shown that Merlin traffics from the plasma membrane with endocytic vesicles in cultured cells (McCartney and Fehon, 1996), raising the possibility that in the absence of Slik, activated Merlin is more stably associated with endocytic compartments than in normal cells. If this is so, inactive Merlin may reside at the plasma membrane and, in response to activation, traffics internally, presumably in association with transmembrane proteins. If this model is correct, it suggests that Merlin may function in tumor suppression by facilitating removal from the plasma membrane of receptors that promote cell proliferation. This model fits well with our recent observation that several receptors, including Notch and the EGF receptor, accumulate to abnormal levels on the surface of cells that are mutant for *Merlin* and the functionally redundant related tumor suppressor *expanded* (Maitra et al., 2006).

Several important questions remain regarding the regulation of Moesin and Merlin that we have described in this study. It remains unclear whether Slik itself can directly phosphorylate either protein or whether there are one or more kinases operating downstream of Slik. Additionally, the dual functions described here may provide novel insights into the role of the mammalian orthologues of Slik, such as PAK, in the malignant transformation of epithelial cells. Equally important will be to elucidate how Slik activity is itself controlled. Given its ability to simultaneously regulate epithelial integrity and proliferation in developing epithelial tissues, Slik may function as a central integrator of the multitude of signals that converge to regulate growth and morphology during development.

Materials and methods

Drosophila stocks

The UAS-*slik* and kinase-inactive *slik* transgenes are described in Hipfner and Cohen (2003). For Slik loss of function analysis in imaginal discs, non-GFP larvae were selected from w^{-}; FRT42D, $slik^{1}$/*CyO, KrGAL4, UAS-GFP* (Hipfner and Cohen, 2003). For overexpression studies, UAS-Myc-Mer^{+} (LaJeunesse et al., 1998), UAS-Myc-Moe^{+}, UAS-Myc-Moe^{T559A}, and UAS-Myc-Moe^{T559D} (Speck et al., 2003) were expressed by crossing to *ap*GAL4 flies (Brand and Perrimon, 1993). A Moesin RNAi transgene

(Karagiosis and Ready, 2004) was crossed to *enGAL4* flies. All other stocks were obtained from the Bloomington Stock Center.

Pulse-chase of Merlin protein in *Drosophila* Schneider cells

S2 cells were cotransfected with either UAS-*slik*$^{+}$ or UAS-*slik*^{kd} and pCasper ubiquitin GAL4 along with pCasper-hs *Mer*$^{+}$ to allow the simultaneous expression of wild-type Slik ubiquitously and a heat shock–driven pulse (30 min at 37°C) of expression of wild-type hsGFP-tagged Merlin (hsMer^{+}). hsMer^{+} retains wild-type function (LaJeunesse et al., 1998). pCasperHS Myc Mer^{T616A} and pCasperHS Myc Mer^{T616D} were made by mutating Thr 616 to alanine or aspartic acid using complementary oligonucleotides and the QuikChange method (Stratagene; constructed by R. Kulikauskas, Duke University, Durham, NC). Mutations were confirmed by sequencing. Cells were collected, fixed in 2% PFA for 20 min at room temperature, and Merlin GFP patterns were analyzed at 1, 3, and 6 h after heat shock. At least three independent replicates were scored for each experiment. For each combination and time point analyzed, a minimum of 150 transfected cells were counted. Myc-tagged constructs were detected using monoclonal anti-Myc at 1:4,000 (9B10; Cell Signaling). Slik was detected using a polyclonal antibody (Hipfner and Cohen, 2003). Myc and Slik were then visualized using cyanine dye CY3, FITC secondary antibodies (Jackson ImmunoResearch Laboratories), and cells mounted in ProLong (Invitrogen). Cells were analyzed using a confocal microscope (LSM510; Carl Zeiss MicroImaging, Inc.) and a plan-Apo 63× NA 1.4 lens.

Immunoblotting and immunolocalization

To characterize the phosphorylation patterns of Merlin protein, late third instar wing imaginal discs were dissected in *Drosophila* serum-free media (Invitrogen) and homogenized in lysis buffer (20 mM Hepes, pH 7.0, 50 mM NaCl, 1 mM EDTA, 0.5 mM EGTA, 10 mM DTT, 1.0% Triton X-100, Complete Protease Inhibitor [Roche], 50 mM NaF, 30 mM Na pyrophosphate, and 100 μm Na orthovanadate). Merlin protein complexes were subsequently immunoprecipitated using guinea pig anti-Merlin linked to Sepharose protein A beads (McCartney and Fehon, 1996) and separated on 8% (118:1) polyacrylamide gels (Scheid et al., 1999). For phosphatase treatment after immunoprecipitation, the protein A beads were precipitated, and one half was then treated with 400 U λ phosphatase (New England Biolabs, Inc.) at 30°C for 45 min followed by Western blot analysis.

Wandering third instar larvae were dissected in serum-free *Drosophila* media and fixed in either 4% PFA or ice-cold 10% TCA (Hayashi et al., 1999) for 20 min. For Western analysis (W) and immunolocalization (I), antibodies used were as follows: guinea pig anti-Slik at 1:40,000 (W) and 1:10,000 (I; provided by S. Cohen and D. Hipfner, European Molecular Biology Laboratory, Heidelberg, Germany), rabbit anti-Moesin D44 at 1:40,000 (W) and 1:20,000 (I; provided by D. Kiehart, Duke University, Durham, NC), rabbit antiphospho-Moesin at 1:10,000 (I; obtained from D. Ready, Purdue University, West Lafayette, IN), guinea pig anti-Merlin at 1:10,000, rhodamine phalloidin at 1:1,000 (Invitrogen), mouse anti-coracle at 1:500, and mouse anti–β-tubulin at 1:5,000 (W; E7; developed by M. Klymkowsky and obtained from the Developmental Studies Hybridoma Bank, The University of Iowa, Iowa City, IO). Appropriate secondary fluorescent antibodies (FITC and cyanine dyes CY3 and CY5) were obtained from Jackson ImmunoResearch Laboratories and were used at 1:1,000. Western blots were visualized and quantified using an infrared imaging system (Odyssey; LI-COR). Immunostained tissues were mounted in ProLong (Invitrogen) and analyzed using either an LSM410 or LSM510 confocal microscope (Carl Zeiss MicroImaging, Inc.) with a plan-Apo 63× NA 1.4 lens. Figures were compiled in Photoshop 7.0.1 (Adobe).

In vitro GST pull-down assay

GST, GST-Merlin, and GST-Moesin fusion proteins were grown in BL21 cells overnight at 37°C. Cultures were diluted 1:100, grown to an OD_{260} of 1, and GST constructs were induced by adding 1 mM IPTG and grown at 18°C for 3 h. Lysates were sonicated and batch incubated with glutathione–Sepharose 4B for 3 h at 4°C and washed in columns with an excess of 10 bed volumes of 1× PBS. [S^{35}]methionine-labeled probe protein (Slik) was prepared using the T7 TNT Quick Coupled Transcription/Translation System (Promega) according to the manufacturer's instructions. Proteins were incubated at 4°C for 4 h and boiled in SDS sample buffer, and proteins were separated on a 10% SDS-PAGE gel, transferred to nitrocellulose, and exposed to film.

Generation of mosaic and MARCM clones

Larvae of the genotype *w; 42DFRT Ubi-GFP^{nls}/42DFRT slik^{1}; hsFLP* or *UAS-CD8-GFP hsFlp; FRT42 Gal80; TubG4/FRT 42D slik^{1}; UAS MYC-Moe^{T559D}* were heat shocked at 36 ± 12 h after egg laying for 1 h at 37°C, 1 h at 25°C, and 1 h at 37°C. Wing imaginal discs were dissected from wandering third instar larval stages and fixed in 4% PFA. GFP was visualized directly. Moesin was detected with rabbit anti-Moesin D44 at 1:20,000 (provided by D. Kiehart), and Merlin was detected with guinea pig anti-Merlin at 1:10,000. Moesin and Merlin were then visualized using cyanine dye CY3 and FITC secondary antibodies, respectively (Jackson ImmunoResearch Laboratories), and cells were mounted in ProLong (Invitrogen). Cells were analyzed using a confocal microscope (LSM510; Carl Zeiss MicroImaging, Inc.) with a plan-Apo 63× NA 1.4 lens.

Wing measurements

Crosses with flies of the appropriate genotypes were raised at 25°C, and wings were analyzed as described previously (LaJeunesse et al., 2001). Images were collected on a camera (AxioCam HRm; Carl Zeiss MicroImaging, Inc.) mounted on a microscope (Axiovert 200M; Carl Zeiss MicroImaging, Inc.) using a Fluar 5× NA 0.25 lens. Area measurements of each wing were obtained from images using the free draw tool in ImageJ software (National Institutes of Health). Statistics were calculated using Excel (Microsoft), and figures were compiled in Photoshop 7.0.1 (Adobe).

We thank A. Neisch, S. Maitra, I. Rebay, A. Simmonds, and members of the Fehon laboratory for comments and critical reading of the manuscript, R. Kulikauskas for Merlin constructs, and D. Hipfner and S. Cohen for Slik reagents. We also thank A. Simmonds for allowing part of this work to be completed in his laboratory.

S.C. Hughes was the recipient of a Young Investigator Award from the Children's Tumor Foundation (formerly known as the National Neurofibromatosis Foundation). This work was funded by grant NS034783 from the National Institutes of Health.

Submitted: 2 August 2006
Accepted: 19 September 2006

References

Bilder, D. 2004. Epithelial polarity and proliferation control: links from the *Drosophila* neoplastic tumor suppressors. *Genes Dev.* 18:1909–1925.

Bilder, D., M. Li, and N. Perrimon. 2000. Cooperative regulation of cell polarity and growth by *Drosophila* tumor suppressors. *Science.* 289:113–116.

Brand, A.H., and N. Perrimon. 1993. Targeted gene expression as a means of altering cell fates and generating dominant phenotypes. *Development.* 118:401–415.

Bretscher, A., K. Edwards, and R.G. Fehon. 2002. ERM proteins and Merlin: integrators at the cell cortex. *Nat. Rev. Mol. Cell Biol.* 3:586–599.

Bryant, P.J., and P. Simpson. 1984. Intrinsic and extrinsic control of growth in developing organs. *Q. Rev. Biol.* 59:387–415.

Condic, M.L., D. Fristrom, and J.W. Fristrom. 1991. Apical cell shape changes during *Drosophila* imaginal leg disc elongation: a novel morphogenetic mechanism. *Development.* 111:23–33.

Dan, I., N.M. Watanabe, and A. Kusumi. 2001. The Ste20 group kinases as regulators of MAP kinase cascades. *Trends Cell Biol.* 11:220–230.

Gary, R., and A. Bretscher. 1995. Ezrin self-association involves binding of an N-terminal domain to a normally masked C-terminal domain that includes the F-actin binding site. *Mol. Biol. Cell.* 6:1061–1075.

Goode, S., and N. Perrimon. 1997. Inhibition of patterned cell shape change and cell invasion by Discs large during *Drosophila* oogenesis. *Genes Dev.* 11:2532–2544.

Gonzalez-Agosti, C., T. Wiederhold, M.E. Herndon, J. Gusella, and V. Ramesh. 1999. Interdomain interaction of Merlin isoforms and its influence on intermolecular binding to NHE-RF. *J. Biol. Chem.* 274:34438–34442.

Gronholm, M., M. Sainio, F. Zhao, L. Heiska, A. Vaheri, and O. Carpen. 1999. Homotypic and heterotypic interaction of the neurofibromatosis 2 tumor suppressor protein Merlin and the ERM protein ezrin. *J. Cell Sci.* 112:895–904.

Gutmann, D.H., L. Sherman, L. Seftor, C. Haipek, K. Hoang Lu, and M. Hendrix. 1999. Increased expression of the NF2 tumor suppressor gene product, Merlin, impairs cell motility, adhesion and spreading. *Hum. Mol. Genet.* 8:267–275.

Hayashi, K., S. Yonemura, T. Matsui, and S. Tsukita. 1999. Immunofluorescence detection of ezrin/radixin/Moesin (ERM) proteins with their carboxyl-terminal threonine phosphorylated in cultured cells and tissues. *J. Cell Sci.* 112:1149–1158.

Hipfner, D.R., and S.M. Cohen. 2003. The *Drosophila* sterile-20 kinase slik controls cell proliferation and apoptosis during imaginal disc development. *PLoS Biol.* 1:E35.

Hipfner, D.R., N. Keller, and S.M. Cohen. 2004. Slik Sterile-20 kinase regulates Moesin activity to promote epithelial integrity during tissue growth. *Genes Dev.* 18:2243–2248.

Irvine, K.D., and E. Wieschaus. 1994. Cell intercalation during *Drosophila* germband extension and its regulation by pair-rule segmentation genes. *Development*. 120:827–841.

Johnston, L.A., and P. Gallant. 2002. Control of growth and organ size in *Drosophila*. *Bioessays*. 24:54–64.

Kalcheim, C., and T. Burstyn-Cohen. 2005. Early stages of neural crest ontogeny: formation and regulation of cell delamination. *Int. J. Dev. Biol.* 49:105–116.

Karagiosis, S.A., and D.F. Ready. 2004. Moesin contributes an essential structural role in *Drosophila* photoreceptor morphogenesis. *Development*. 131:725–732.

Kissil, J.L., K.C. Johnson, M.S. Eckman, and T. Jacks. 2002. Merlin phosphorylation by p21-activated kinase 2 and effects of phosphorylation on Merlin localization. *J. Biol. Chem.* 277:10394–10399.

LaJeunesse, D.R., B.M. McCartney, and R.G. Fehon. 1998. Structural analysis of *Drosophila* Merlin reveals functional domains important for growth control and subcellular localization. *J. Cell Biol.* 141:1589–1599.

LaJeunesse, D.R., B.M. McCartney, and R.G. Fehon. 2001. A systematic screen for dominant second-site modifiers of Merlin/NF2 phenotypes reveals an interaction with blistered/DSRF and scribbler. *Genetics*. 158:667–679.

Maitra, S., R.M. Kulikauskas, H. Gavilan, and R.G. Fehon. 2006. The tumor suppressors Merlin and expanded function cooperatively to modulate receptor endocytosis and signaling. *Curr. Biol.* 16:702–709.

Matsui, T., M. Maeda, Y. Doi, S. Yonemura, M. Amano, K. Kaibuchi, and S. Tsukita. 1998. Rho-kinase phosphorylates COOH-terminal threonines of ezrin/radixin/Moesin (ERM) proteins and regulates their head-to-tail association. *J. Cell Biol.* 140:647–657.

McCartney, B.M., and R.G. Fehon. 1996. Distinct cellular and subcellular patterns of expression imply distinct functions for the *Drosophila* homologues of Moesin and the neurofibromatosis 2 tumor suppressor, Merlin. *J. Cell Biol.* 133:843–852.

Meng, J.J., D.J. Lowrie, H. Sun, E. Dorsey, P.D. Pelton, A.M. Bashour, J. Groden, N. Ratner, and W. Ip. 2000. Interaction between two isoforms of the NF2 tumor suppressor protein, Merlin, and between Merlin and ezrin, suggests modulation of ERM proteins by Merlin. *J. Neurosci. Res.* 62:491–502.

Morrison, H., L.S. Sherman, J. Legg, F. Banine, C. Isacke, C.A. Haipek, D.H. Gutmann, H. Ponta, and P. Herrlich. 2001. The NF2 tumor suppressor gene product, Merlin, mediates contact inhibition of growth through interactions with CD44. *Genes Dev.* 15:968–980.

Nakamura, F., M.R. Amieva, and H. Furthmayr. 1995. Phosphorylation of threonine 558 in the carboxyl-terminal actin-binding domain of Moesin by thrombin activation of human platelets. *J. Biol. Chem.* 270:31377–31385.

Nakamura, F., L. Huang, K. Pestonjamasp, E.J. Luna, and H. Furthmayr. 1999. Regulation of F-actin binding to platelet Moesin in vitro by both phosphorylation of threonine 558 and polyphosphatidylinositides. *Mol. Biol. Cell*. 10:2669–2685.

Nguyen, R., D. Reczek, and A. Bretscher. 2001. Hierarchy of Merlin and ezrin N- and C-terminal domain interactions in homo- and heterotypic associations and their relationship to binding of scaffolding proteins EBP50 and E3KARP. *J. Biol. Chem.* 276:7621–7629.

Oshiro, N., Y. Fukata, and K. Kaibuchi. 1998. Phosphorylation of Moesin by rho-associated kinase (Rho-kinase) plays a crucial role in the formation of microvilli-like structures. *J. Biol. Chem.* 273:34663–34666.

Rouleau, G.A., P. Merel, M. Lutchman, M. Sanson, J. Zucman, C. Marineau, K. Hoang-Xuan, S. Demczuk, C. Desmaze, B. Plougastel, et al. 1993. Alteration in a new gene encoding a putative membrane-organizing protein causes neuro-fibromatosis type 2. *Nature*. 363:515–521.

Scheid, M.P., K.M. Schubert, and V. Duronio. 1999. Regulation of bad phosphorylation and association with Bcl-x(L) by the MAPK/Erk kinase. *J. Biol. Chem.* 274:31108–31113.

Scherer, S.S., and D.H. Gutmann. 1996. Expression of the neurofibromatosis 2 tumor suppressor gene product, Merlin, in Schwann cells. *J. Neurosci. Res.* 46:595–605.

Schmucker, B., W.G. Ballhausen, and M. Kressel. 1997. Subcellular localization and expression pattern of the neurofibromatosis type 2 protein Merlin/schwannomin. *Eur. J. Cell Biol.* 72:46–53.

Shaw, R.J., A.I. McClatchey, and T. Jacks. 1998. Regulation of the neurofibromatosis type 2 tumor suppressor protein, Merlin, by adhesion and growth arrest stimuli. *J. Biol. Chem.* 273:7757–7764.

Shaw, R.J., J.G. Paez, M. Curto, A. Yaktine, W.M. Pruitt, I. Saotome, J.P. O'Bryan, V. Gupta, N. Ratner, C.J. Der, et al. 2001. The Nf2 tumor suppressor, Merlin, functions in Rac-dependent signaling. *Dev. Cell*. 1:63–72.

Sherman, L., H.M. Xu, R.T. Geist, S. Saporito-Irwin, N. Howells, H. Ponta, P. Herrlich, and D.H. Gutmann. 1997. Interdomain binding mediates tumor growth suppression by the NF2 gene product. *Oncogene*. 15:2505–2509.

Speck, O., S.C. Hughes, N.K. Noren, R.M. Kulikauskas, and R.G. Fehon. 2003. Moesin functions antagonistically to the Rho pathway to maintain epithelial integrity. *Nature*. 421:83–87.

Surace, E.I., C.A. Haipek, and D.H. Gutmann. 2004. Effect of Merlin phosphorylation on neurofibromatosis 2 (NF2) gene function. *Oncogene*. 23:580–587.

Tran Quang, C., A. Gautreau, M. Arpin, and R. Treisman. 2000. Ezrin function is required for ROCK-mediated fibroblast transformation by the net and dbl oncogenes. *EMBO J.* 19:4565–4576.

Trofatter, J.A., M.M. MacCollin, J.L. Rutter, J.R. Murrell, M.P. Duyao, D.M. Parry, R. Eldridge, N. Kley, A.G. Menon, K. Pulaski, et al. 1993a. A novel Moesin-, ezrin-, radixin-like gene is a candidate for the neurofibromatosis 2 tumor suppressor. *Cell*. 75:826. (published erratum appears in *Cell.* 1993. 72:791–800.

Trofatter, J.A., M.M. MacCollin, J.L. Rutter, J.R. Murrell, M.P. Duyao, D.M. Parry, R. Eldridge, N. Kley, A.G. Menon, K. Pulaski, et al. 1993b. A novel Moesin-, ezrin-, radixin-like gene is a candidate for the neurofibromatosis 2 tumor suppressor. *Cell*. 72:791–800.

Xiao, G.H., A. Beeser, J. Chernoff, and J.R. Testa. 2002. p21-activated kinase links Rac/Cdc42 signaling to Merlin. *J. Biol. Chem.* 277:883–886.

Zeitler, J., C.P. Hsu, H. Dionne, and D. Bilder. 2004. Domains controlling cell polarity and proliferation in the *Drosophila* tumor suppressor Scribble. *J. Cell Biol.* 167:1137–1146.